EUROPEAN ORGANIZATION FOR NUCLEAR RESEARCH

CERN PPE/93-214
December 16, 1993

Measurement of the B_s^0 Lifetime

The ALEPH Collaboration*

Abstract

The lifetime of the B_s^0 has been measured in a data sample of 889,000 hadronic events recorded with the ALEPH detector at LEP. After background subtraction 30.8 ± 6.9 events are attributed to the semileptonic decay of the B_s^0 to a D_s^- and an opposite-sign lepton. A maximum-likelihood fit to the distribution of the proper times of these events yields a B_s^0 lifetime of :

$$\tau_{B_s} = 1.92^{+0.45}_{-0.35} \pm 0.04 \text{ ps}.$$

(Submitted to Physics Letters B)

*See the following pages for the list of authors.

The ALEPH Collaboration

D. Buskulic, I. De Bonis, D. Decamp, P. Ghez, C. Goy, J.-P. Lees, M.-N. Minard, P. Odier, B. Pietrzyk

Laboratoire de Physique des Particules (LAPP), IN^{2}P^3-CNRS, 74019 Annecy-le-Vieux Cedex, France

F. Ariztizabal, P. Comas, J.M. Crespo, I. Efthymiopoulos, E. Fernandez, M. Fernandez-Bosman, V. Gaitan, Ll. Garrido,[29] M. Martinez, T. Mattison,[30] S. Orteu, A. Pacheco, C. Padilla, A. Pascual

Institut de Fisica d'Altes Energies, Universitat Autonoma de Barcelona, 08193 Bellaterra (Barcelona), Spain[7]

D. Creanza, M. de Palma, A. Farilla, G. Iaselli, G. Maggi, N. Marinelli, S. Natali, S. Nuzzo, A. Ranieri, G. Raso, F. Romano, F. Ruggieri, G. Selvaggi, L. Silvestris, P. Tempesta, G. Zito

Dipartimento di Fisica, INFN Sezione di Bari, 70126 Bari, Italy

Y. Chai, H. Hu, D. Huang, X. Huang, J. Lin, T. Wang, Y. Xie, D. Xu, R. Xu, J. Zhang, L. Zhang, W. Zhao

Institute of High-Energy Physics, Academia Sinica, Beijing, The People's Republic of China[8]

G. Bonvicini, J. Boudreau, D. Casper, H. Drevermann, R.W. Forty, G. Ganis, C. Gay, M. Girone, R. Hagelberg, J. Harvey, J. Hilgart,[27] R. Jacobsen, B. Jost, J. Knobloch, I. Lehraus, M. Maggi, C. Markou, P. Mato, H. Meinhard, A. Minten, R. Miquel, H.-G. Moser, P. Palazzi, J.R. Pater, J.A. Perlas, P. Perrodo, J.-F. Pusztaszeri, F. Ranjard, L. Rolandi, J. Rothberg,[2] T. Ruan, M. Saich, D. Schlatter, M. Schmelling, F. Sefkow,[6] W. Tejessy, I.R. Tomalin, R. Veenhof, H. Wachsmuth, S. Wasserbaech,[2] W. Wiedenmann, T. Wildish, W. Witzeling, J. Wotschack

European Laboratory for Particle Physics (CERN), 1211 Geneva 23, Switzerland

Z. Ajaltouni, M. Bardadin-Otwinowska, A. Barres, C. Boyer, A. Falvard, P. Gay, C. Guicheney, P. Henrard, J. Jousset, B. Michel, J-C. Montret, D. Pallin, P. Perret, F. Podlyski, J. Proriol, F. Saadi

Laboratoire de Physique Corpusculaire, Université Blaise Pascal, IN^{2}P^3-CNRS, Clermont-Ferrand, 63177 Aubière, France

T. Fearnley, J.B. Hansen, J.D. Hansen, J.R. Hansen, P.H. Hansen, S.D. Johnson, R. Møllerud, B.S. Nilsson[1]

Niels Bohr Institute, 2100 Copenhagen, Denmark[9]

A. Kyriakis, E. Simopoulou, I. Siotis, A. Vayaki, K. Zachariadou

Nuclear Research Center Demokritos (NRCD), Athens, Greece

J. Badier, A. Blondel, G. Bonneaud, J.C. Brient, P. Bourdon, G. Fouque, L. Passalacqua, A. Rougé, M. Rumpf, R. Tanaka, M. Verderi, H. Videau

Laboratoire de Physique Nucléaire et des Hautes Energies, Ecole Polytechnique, IN^{2}P^3-CNRS, 91128 Palaiseau Cedex, France

D.J. Candlin, M.I. Parsons, E. Veitch

Department of Physics, University of Edinburgh, Edinburgh EH9 3JZ, United Kingdom[10]

E. Focardi, L. Moneta, G. Parrini

Dipartimento di Fisica, Università di Firenze, INFN Sezione di Firenze, 50125 Firenze, Italy

M. Corden, M. Delfino,[12] C. Georgiopoulos, D.E. Jaffe, D. Levinthal[15]

Supercomputer Computations Research Institute, Florida State University, Tallahassee, FL 32306-4052, USA [13,14]

A. Antonelli, G. Bencivenni, G. Bologna,[4] F. Bossi, P. Campana, G. Capon, F. Cerutti, V. Chiarella, G. Felici, P. Laurelli, G. Mannocchi,[5] F. Murtas, G.P. Murtas, M. Pepe-Altarelli, S. Salomone

Laboratori Nazionali dell'INFN (LNF-INFN), 00044 Frascati, Italy

P. Colrain, I. ten Have, I.G. Knowles, J.G. Lynch, W. Maitland, W.T. Morton, C. Raine, P. Reeves, J.M. Scarr, K. Smith, M.G. Smith, A.S. Thompson, S. Thorn, R.M. Turnbull

Department of Physics and Astronomy, University of Glasgow, Glasgow G12 8QQ,United Kingdom[10]

B. Brandl, O. Braun, C. Geweniger, G. Graefe, P. Hanke, V. Hepp, C. Karger, E.E. Kluge, Y. Maumary, A. Putzer,[1] B. Rensch, A. Stahl, K. Tittel, M. Wunsch

Institut für Hochenergiephysik, Universität Heidelberg, 69120 Heidelberg, Fed. Rep. of Germany[16]

R. Beuselinck, D.M. Binnie, W. Cameron, M. Cattaneo, D.J. Colling, P.J. Dornan, J.F. Hassard, N.M. Lieske,[25] A. Moutoussi, J. Nash, S. Patton, D.G. Payne, M.J. Phillips, G. San Martin, J.K. Sedgbeer, A.G. Wright

Department of Physics, Imperial College, London SW7 2BZ, United Kingdom[10]

P. Girtler, D. Kuhn, G. Rudolph, R. Vogl

Institut für Experimentalphysik, Universität Innsbruck, 6020 Innsbruck, Austria[18]

C.K. Bowdery, T.J. Brodbeck, A.J. Finch, F. Foster, G. Hughes, D. Jackson, N.R. Keemer, M. Nuttall, A. Patel, T. Sloan, S.W. Snow, E.P. Whelan

Department of Physics, University of Lancaster, Lancaster LA1 4YB, United Kingdom[10]

A. Galla, A.M. Greene, K. Kleinknecht, J. Raab, B. Renk, H.-G. Sander, H. Schmidt, S.M. Walther, R. Wanke, B. Wolf

Institut für Physik, Universität Mainz, 55099 Mainz, Fed. Rep. of Germany[16]

A.M. Bencheikh, C. Benchouk, A. Bonissent, D. Calvet, J. Carr, P. Coyle, C. Diaconu, J. Drinkard,[3] F. Etienne, D. Nicod, P. Payre, L. Roos, D. Rousseau, P. Schwemling, M. Talby

Centre de Physique des Particules, Faculté des Sciences de Luminy, IN^{2}P^3-CNRS, 13288 Marseille, France

S. Adlung, R. Assmann, C. Bauer, W. Blum, D. Brown, P. Cattaneo,[23] B. Dehning, H. Dietl, F. Dydak,[21] M. Frank, A.W. Halley, K. Jakobs, J. Lauber, G. Lütjens, G. Lutz, W. Männer, R. Richter, J. Schröder, A.S. Schwarz, R. Settles, H. Seywerd, U. Stierlin, U. Stiegler, R. St. Denis, G. Wolf

Max-Planck-Institut für Physik, Werner-Heisenberg-Institut, 80805 München, Fed. Rep. of Germany[16]

R. Alemany, J. Boucrot,[1] O. Callot, A. Cordier, M. Davier, L. Duflot, J.-F. Grivaz, Ph. Heusse, P. Janot, D.W. Kim,[19] F. Le Diberder, J. Lefrançois, A.-M. Lutz, G. Musolino, M.-H. Schune, J.-J. Veillet, I. Videau

Laboratoire de l'Accélérateur Linéaire, Université de Paris-Sud, IN^{2}P^3-CNRS, 91405 Orsay Cedex, France

D. Abbaneo, G. Bagliesi, G. Batignani, U. Bottigli, C. Bozzi, G. Calderini, M. Carpinelli, M.A. Ciocci, V. Ciulli, R. Dell'Orso, I. Ferrante, F. Fidecaro, L. Foà, F. Forti, A. Giassi, M.A. Giorgi, A. Gregorio, F. Ligabue, A. Lusiani, E.B. Mannelli, P.S. Marrocchesi, A. Messineo, F. Palla, G. Rizzo, G. Sanguinetti, P. Spagnolo, J. Steinberger, R. Tenchini,[1] G. Tonelli,[28] G. Triggiani, A. Valassi, C. Vannini, A. Venturi, P.G. Verdini, J. Walsh

Dipartimento di Fisica dell'Università, INFN Sezione di Pisa, e Scuola Normale Superiore, 56010 Pisa, Italy

A.P. Betteridge, Y. Gao, M.G. Green, D.L. Johnson, P.V. March, T. Medcalf, Ll.M. Mir, I.S. Quazi, J.A. Strong

Department of Physics, Royal Holloway & Bedford New College, University of London, Surrey TW20 OEX, United Kingdom[10]

V. Bertin, D.R. Botterill, R.W. Clifft, T.R. Edgecock, S. Haywood, M. Edwards, P.R. Norton, J.C. Thompson

Particle Physics Dept., Rutherford Appleton Laboratory, Chilton, Didcot, Oxon OX11 OQX, United Kingdom[10]

B. Bloch-Devaux, P. Colas, H. Duarte, S. Emery, W. Kozanecki, E. Lançon, M.C. Lemaire, E. Locci, B. Marx, P. Perez, J. Rander, J.-F. Renardy, A. Rosowsky, A. Roussarie, J.-P. Schuller, J. Schwindling, D. Si Mohand, B. Vallage

Service de Physique des Particules, DAPNIA, CE-Saclay, 91191 Gif-sur-Yvette Cedex, France[17]

R.P. Johnson, A.M. Litke, G. Taylor, J. Wear

Institute for Particle Physics, University of California at Santa Cruz, Santa Cruz, CA 95064, USA[22]

W. Babbage, C.N. Booth, C. Buttar, S. Cartwright, F. Combley, I. Dawson, L.F. Thompson

Department of Physics, University of Sheffield, Sheffield S3 7RH, United Kingdom[10]

E. Barberio,[31] A. Böhrer, S. Brandt, G. Cowan,[1] C. Grupen, G. Lutters, F. Rivera,[26] U. Schäfer, L. Smolik

Fachbereich Physik, Universität Siegen, 57068 Siegen, Fed. Rep. of Germany[16]

L. Bosisio, R. Della Marina, G. Giannini, B. Gobbo, L. Pitis, F. Ragusa[20]

Dipartimento di Fisica, Università di Trieste e INFN Sezione di Trieste, 34127 Trieste, Italy

L. Bellantoni, W. Chen, J.S. Conway,[24] Z. Feng, D.P.S. Ferguson, Y.S. Gao, J. Grahl, J.L. Harton, O.J. Hayes III, J.M. Nachtman, Y.B. Pan, Y. Saadi, M. Schmitt, I. Scott, V. Sharma, Z.H. Shi, J.D. Turk, A.M. Walsh, F.V. Weber, Sau Lan Wu, X. Wu, M. Zheng, G. Zobernig

Department of Physics, University of Wisconsin, Madison, WI 53706, USA[11]

---

[1] Now at CERN, PPE Division, 1211 Geneva 23, Switzerland.
[2] Permanent address: University of Washington, Seattle, WA 98195, USA.
[3] Now at University of California, Irvine, CA 92717, USA.
[4] Also Istituto di Fisica Generale, Università di Torino, Torino, Italy.
[5] Also Istituto di Cosmo-Geofisica del C.N.R., Torino, Italy.
[6] Now at DESY, Hamburg, Germany.
[7] Supported by CICYT, Spain.
[8] Supported by the National Science Foundation of China.
[9] Supported by the Danish Natural Science Research Council.
[10] Supported by the UK Science and Engineering Research Council.
[11] Supported by the US Department of Energy, contract DE-AC02-76ER00881.
[12] On leave from Universitat Autonoma de Barcelona, Barcelona, Spain.
[13] Supported by the US Department of Energy, contract DE-FG05-92ER40742.
[14] Supported by the US Department of Energy, contract DE-FC05-85ER250000.
[15] Present address: Lion Valley Vineyards, Cornelius, Oregon, U.S.A.
[16] Supported by the Bundesministerium für Forschung und Technologie, Fed. Rep. of Germany.
[17] Supported by the Direction des Sciences de la Matière, C.E.A.
[18] Supported by Fonds zur Förderung der wissenschaftlichen Forschung, Austria.
[19] Permanent address: Kangnung National University, Kangnung, Korea.
[20] Now at Dipartimento di Fisica, Università di Milano, Milano, Italy.
[21] Also at CERN, PPE Division, 1211 Geneva 23, Switzerland.
[22] Supported by the US Department of Energy, grant DE-FG03-92ER40689.
[23] Now at Università di Pavia, Pavia, Italy.
[24] Now at Rutgers University, Piscataway, NJ 08854, USA.
[25] Now at Oxford University, Oxford OX1 3RH, U.K.
[26] Partially supported by Colciencias, Colombia.
[27] Now at SSCL, Dallas 75237-3946, TX, U.S.A.
[28] Also at Istituto di Matematica e Fisica, Università di Sassari, Sassari, Italy.
[29] Permanent address: Dept. d'Estructura i Constituens de la Materia, Universitat de Barcelona, 08208 Barcelona, Spain.
[30] Now at SLAC, Stanford, CA 94309, U.S.A.
[31] Now at Università della Calabria, Cosenza, Italy.

1 Introduction

Measurements of the individual lifetimes of the b hadrons enable quantitative testing of the importance of non-spectator contributions, Pauli exclusion effects and final state interactions in b hadron decays. For charmed hadrons such effects have been observed to be large (e.g. $\tau_{D^+}/\tau_{D^0} = 2.54 \pm 0.07$ [1]). In the case of b hadrons, due to the larger mass of the b quark, lifetime differences up to $15\% - 20\%$ between the b hadrons are expected [2, 3].

The B_s^0 has been observed via its semileptonic decays [4, 5, 6] and its mass has been precisely measured in a small number of fully reconstructed hadronic decays [7, 8]. The technique used in this measurement of the B_s^0 lifetime is based on three-dimensional vertexing of the fully reconstructed D_s^- and the lepton originating from the $B_s^0 \to D_s^- l^+ \nu$ semileptonic decay[1].

The following sections describe the ALEPH detector, the selection of the events, the measurement of the decay length, the procedure of estimating the boost in the presence of the neutrino, the fitting method and finally results and systematic errors.

2 The ALEPH Detector and Lepton Identification

The ALEPH detector is described in detail in reference [9]. Only a brief description of the apparatus is given here.

Charged particles are tracked with three devices inside a superconducting solenoid providing an axial field of 1.5 T. Closest to the beampipe is the vertex detector (VDET) [10], installed in 1991, which consists of silicon wafers with strip readout in two dimensions, arranged in two cylindrical layers at average radii of 6.3 and 10.8 cm. This detector covers an angular range down to $|\cos\theta| < 0.85$ for the inner layer only and $|\cos\theta| < 0.69$ with both layers. The point resolution is 12 μm at normal incidence in the $r\phi$ and rz dimensions. Surrounding the VDET is the inner tracking chamber (ITC), a drift chamber giving up to eight measurements in the $r\phi$ dimension. Outside the ITC, the time projection chamber (TPC) provides up to 21 space points for $|\cos\theta| < 0.79$, and a decreasing number for smaller angles, with four points at $|\cos\theta| = 0.96$. With this combined system a momentum resolution of $\Delta p/p = 0.0006\ p\ (\mathrm{GeV}/c)^{-1}$ is obtained for 45 GeV/c muons. The TPC also provides up to 330 measurements of the specific ionization of each charged track, with a measured $\mathrm{d}E/\mathrm{d}x$ resolution of 4.5% for Bhabba electrons having 330 ionization samples. For charged particles with momenta above 3 GeV/c, the (60% truncated) mean specific ionization of pions and that of kaons are typically separated by two standard deviations.

Lepton identification in ALEPH is described in detail elsewhere [11]. Electrons are identified using the electromagnetic calorimeter (ECAL) and the TPC. The ECAL is a lead wire-chamber sandwich operated in proportional mode with cathode-pads readout in $0.8^\circ \times 0.8^\circ$ projective towers segmented in three longitudinal stacks. Electrons are identified by comparing the momentum measured in the TPC with the energy measured in the four ECAL towers closest to the track extrapolation, by checking the consistency

[1] Charge conjugate reactions are implied throughout this letter.

of the depth of the ECAL shower with that expected for an electron, and by rejecting particles with a mean specific ionization more than 2.5 standard deviations below the expectation for an electron. Electron candidates identified as coming from photon conversions using the algorithm described in reference [11] are rejected.

Muons are identified using the hadron calorimeter (HCAL) and the muon chambers. The HCAL is composed of the iron of the magnet return yoke interleaved with 23 layers of streamer tubes. The readout of the HCAL consists of strips with a pitch of 1 cm which are used for the muon tracking, and $3° \times 3°$ projective towers used for the hadronic energy measurement. The muon chambers surround the HCAL after a total of 7.5 interaction lengths of material and consist of four layers of streamer tubes, which provide three dimensional information on the position of a hit. For this analysis, muon candidates are accepted if they have a hit pattern characteristic of a penetrating particle in the HCAL or if they have at least two associated hits in the muon chambers.

3 Event Selection and Backgrounds

The B_s^0 is isolated using the following decays (figure 1):

$$\begin{aligned} B_s^0 &\longrightarrow D_s^- \ell^+ \nu \\ &\quad \hookrightarrow \phi\pi^- \\ &\quad\quad \hookrightarrow K^+K^- \end{aligned}$$

and

$$\begin{aligned} B_s^0 &\longrightarrow D_s^- \ell^+ \nu \\ &\quad \hookrightarrow K^{*0}K^- \\ &\quad\quad \hookrightarrow K^+\pi^- \end{aligned}$$

where the lepton is an identified electron or a muon and is required to have a momentum greater than 3 GeV/c. The π^- and the K^- coming directly from the D_s^- decay are referred to as 'bachelor' particles to distinguish them from those of the K^{*0} and ϕ decays.

A total of 889,000 hadronic Z decays recorded in 1991 and 1992 are used in this analysis. The $D_s^-\ell^+$ selection is similar to that used in a previous letter [5] with the addition of requirements on the track quality and vertexing needed for the decay length measurement.

Each event is divided into two hemispheres separated by the plane perpendicular to the thrust axis. Candidates for decay of the D_s^- into $\phi\pi^-$ or $K^{*0}K^-$ are formed by combining three charged tracks with momenta above 1 GeV/c in the same hemisphere. As backgrounds are higher in the $D_s^- \to K^*K^-$ case, the bachelor kaon momentum is required to be greater than 2 GeV/c. Out of these three tracks, a neutral pair is required to be consistent with a ϕ or a K^{*0} by demanding either the K^+K^- mass to be within ± 9 MeV/c^2 of the ϕ mass or the $K^+\pi^-$ mass to be within ± 50 MeV/c^2 of the $K^{*0}(892)$ mass. The ϕ or K^{*0} momentum has to be greater than 4 GeV/c and the D_s^- energy greater than 15% of the beam energy. In addition the $KK\pi l$ mass is required to be greater than 3 GeV/c^2. These requirements reduce the combinatorial background from low-momentum fragmentation tracks, reduce physics backgrounds

from non-B_s^0 sources and restrict the candidate tracks to a momentum range where the π/K-separation from the TPC $\mathrm{d}E/\mathrm{d}x$ measurement is at the two standard deviation level. When ionization information is available, kaon candidates are required to fulfil $\chi_K < 1-\chi_\pi$, where χ_H is the difference between the measured and expected ionization expressed in terms of standard deviations for mass hypothesis H. Compared to the usual two standard deviation cut on χ_K this cut improves the pion rejection by a factor 1.5 with only a 4% loss of efficiency. For the bachelor kaon from the K^*K^- decay the combination is rejected if ionization information is not available (18% of the cases).

Further background reduction is obtained by using the angular distributions in the subsequent decay chain. As the D_s^- is spinless, its decay is expected to be isotropic, whereas the background, consisting of more asymmetric random track combinations, gives a decay angular distribution peaking in the forward and backward directions. The cosine of the decay angle in the D_s^- centre-of-mass frame $|cos\theta^*(\phi)|$ or $|cos\theta^*(K^*)|$ is thus required to be less than 0.8. As the D_s^- decays to a vector (ϕ or K^{*0}) and a pseudoscalar (π^- or K^-), the subsequent decay of the vector to two pseudoscalars (KK or $K\pi$) will have a $cos^2\lambda^*$ distribution, where λ^* is the centre-of-mass decay angle of the vector particle relative to its line of flight. In contrast, the background measured in data is observed to be uniform. A cut at $|cos\lambda^*(K/\phi)|$ and $|cos\lambda^*(K/K^*)|$ greater than 0.5 is 88% efficient for the signal, while removing half of the background.

In order to ensure good vertex reconstruction and to reduce the non-Gaussian tails in the decay-length measurement, the lepton track and at least two of the tracks from the D_s^- decay are required to have one or more associated vertex detector hits. The χ^2 probability of the three tracks forming the D_s^- candidate to come from a single three-dimensional vertex is required to be greater than 1%. The same requirement is also made on the χ^2 probability of the D_s^- and the lepton to form a single vertex.

Figure 2 shows the histogram of the $KK\pi$ effective mass for the opposite-sign and same-sign $D_s\ell$ correlations summed over the $\phi\pi^-$ and $K^{*0}K^-$ channels. A clear peak at a mass of 1.9677 ± 0.0015 GeV/c^2, consistent with the D_s^-, can be seen in the opposite-sign correlation plot. In the same-sign plot no such peak is observed. Within ± 15 MeV/c^2 of the D_s^- mass, 47 events (16 in the $\phi\pi^-$ channel and 31 in the $K^{*0}K^-$ channel) are found and used for the lifetime measurement.

A source of background which is expected to show a structure in the mass distribution around the D_s^- mass in the $K^{*0}K^-$ channel, is the reflection of the $D^- \to K^{*0}\pi^-$ decay due to misidentification of the π^- as a K^-. In this case the D^- is produced in association with an opposite-sign lepton in the decay $B \to D^- X\ell^+\nu$. This background is estimated to be 0.5 ± 0.2 events, using $BR(B \to D^- X\ell^+\nu) = (4.0\pm0.6)\%$ and the efficiencies obtained from the Monte Carlo simulation. As a check, the rate for $D^\pm$ is also obtained from the 5 ± 3 events observed in the D^- region of the $KK\pi$ mass distribution due to the Cabibbo-suppressed decay modes $D^- \to \phi\pi^-$ or $K^{*0}K^-$. Correcting this number by the appropriate branching ratios and relative efficiencies leads to an estimate of 0.5 ± 0.3 events reflecting as $D_s \to K^*K$, in agreement with the previous estimate.

The combinatorial background under the peak is estimated by fitting a polynomial to the side bands of the opposite-sign correlation mass distribution between 1.7 and

Component	Number of Events
Observed events	47
Combinatorial background	11.9 ± 0.9
$D_s D$ background	3.8 ± 0.6
Reflection background	0.5 ± 0.2
Total background	16.2 ± 1.1
Signal	30.8 ± 6.9

Table 1: Signal and background estimates within ± 15 MeV/c^2 of the D_s^- mass.

2.2 GeV/c^2. The mass regions $m(D^+) \pm 20$ MeV/c^2 and 1.94 GeV/c^2 $< m(KK\pi) <$ 2.02 GeV/c^2 are excluded from the side bands in order to avoid regions where the D^- signal and its reflection are expected. The estimated background is 11.9 ± 0.9 events (3.5 in the $\phi\pi^-$ channel and 8.5 in the $K^{*0}K^-$ channel).

Genuine D_s^-s from non-B_s^0 sources can also lead to an opposite-sign $D_s^-\ell^+$ correlation. These backgrounds have been discussed in detail in reference [5] and are briefly summarized here.

$$\bar{B} \to D_s^{(*)-} D^{(*)} X, \quad D^{(*)} \to \ell^+ \nu X \tag{1}$$

$$B \to D_s^{(*)-} X_s \ell^+ \nu \tag{2}$$

Process (1) is the decay of B_d or B_u into states containing two charmed particles. Using the measurement of the product branching ratio $BR(B \to D_s X) BR(D_s \to \phi\pi) = (3.0 \pm 0.34) \times 10^{-3}$ averaged from references [12] and [13], semileptonic branching ratios of D^+ and D^0 from [1] and efficiencies obtained from Monte Carlo simulation of the $\phi\pi$ and the $K^{*0}K$ channels, a total of 3.8 ± 0.6 events are expected in the final sample. Process (2) is the semileptonic decay of a non-strange B meson to a hadronic system including a D_s and a hadronic system X_s carrying opposite strangeness. To date this decay has not been observed [14], but a theoretical analysis [15] yields the limit $BR(B_d, B^+ \to D_s X_s \ell\nu) < 0.025 \times BR(B_d \to X\ell\nu)$. As this background is expected to be very small, it is not explicitly included in the lifetime fit. The effect of its possible presence is taken into account in the systematic error. Table 1 summarizes the signal and background estimates for the B_s^0 selection.

4 Proper-Time Measurement

The proper time (t) and its error are obtained for each event from the decay length (l) and momentum (p_{B_s}) of the B_s^0 candidate using $t = \frac{l m_{B_s}}{p_{B_s} c}$ where m_{B_s} is the B_s^0 mass. The decay length is calculated by projecting the vector joining the interaction point and the B_s^0 decay vertex onto the B_s^0 flight direction as estimated from the D_s-lepton system [16].

The method used to reconstruct the event-by-event interaction point is made insensitive to the lifetime information of the tracks by projecting them onto the plane perpendicular to the jet to which they belong and combines this with the envelope of the luminous region. The centre of the luminous region is periodically determined from hadronic events reconstructed and analysed over 75 successive events. Using this algorithm on simulated $b\bar{b}$ events the average resolution on the position of the interaction point projected along the sphericity axis of the event is 85 μm.

The position of the B_s^0 vertex is measured in three dimensions by first vertexing the three charged tracks from the decay of the D_s^- and then extrapolating the D_s^- track to its intersection with the lepton as shown in figure 1. The resolutions along the direction of flight obtained in simulated events are 320 μm for the D_s^- vertex and 210 μm for the B_s^0 vertex.

The error on the decay length is calculated for each event from the tracking and vertexing errors. To determine how well this error and thus the proper time uncertainty is estimated, a resolution function is formed using the Monte Carlo simulation by fitting with a Gaussian the distribution of the difference between the reconstructed and true decay length divided by the uncertainty on the reconstructed decay length. This distribution is centred at zero and is well represented by a single Gaussian of sigma $S = 1.21 \pm 0.05$, indicating that the decay length uncertainty is underestimated. To take this into account in the lifetime fit, the calculated decay length error is scaled by S. Possible differences between Monte Carlo and real data for this quantity are considered in the systematic error.

The B_s^0 momentum is calculated as

$$p_{B_s}^2 = (E_{D_s} + E_\ell + E_\nu)^2 - m_{B_s}^2,$$

where E_{D_s} and E_ℓ are the measured energies of the D_s^- and the lepton respectively. The neutrino energy (E_ν) is estimated using a missing energy technique. It is given by

$$E_\nu = E_{tot} - E_{vis},$$

where E_{tot} and E_{vis} are the total and visible energies in the same hemisphere as the B_s^0 candidate. The visible energy is obtained by summing the energies of the charged particles measured by the tracking detectors and the photons measured by the electromagnetic calorimeter. The small contribution from the neutral hadronic energy, which has a large measurement uncertainty, is not included. Using four-momentum conservation the total energy in the hemisphere is given by

$$E_{tot} = E_{beam} + \frac{m_{same}^2 - m_{opp}^2}{4E_{beam}}$$

where E_{beam} is the beam energy and the hemisphere masses on the same side (m_{same}) and opposite side (m_{opp}) of the B_s^0 candidate are calculated using the momenta of the photons and charged tracks measured in the appropriate hemisphere. Monte Carlo simulation shows that the addition of the hemisphere mass correction term to the beam energy improves the resolution on E_{tot} from 2.5 GeV to 1.3 GeV and yields a resolution on the neutrino energy of 2.8 GeV.

The final resolution obtained for the B_s^0 momentum using this method is displayed in figure 3 which shows the distribution of the ratio (κ) of the reconstructed B_s^0 momentum divided by the true B_s^0 momentum for simulated B_s^0 events. The presence of D_s^- originating from a D_s^{*-} with the emission of a soft photon is included in Monte Carlo simulation assuming a value of 3.0 for the ratio $\frac{BR(B_s \to D_s^* l\nu)}{BR(B_s \to D_s l\nu)}$. The mean of the κ distribution is 1.05 and the r.m.s is 11.5% with about 85% of the events contained within a Gaussian core of sigma 5%. To correct for the shift from 1.0 and the non-Gaussian tail in this distribution, mainly due to energy losses, the κ distribution is used in the fitting procedure.

5 Fitting Procedure

The B_s^0 lifetime and the proper-time structure of the combinatorial background are fitted simultaneously to the events in the peak and the side bands by maximizing the following unbinned likelihood function:

$$\mathcal{L} = \prod_{i=1}^{n_{peak}} \mathcal{P}_{peak}(t_i, S\sigma_{t_i}) \prod_{j=1}^{n_{side}} \mathcal{P}_{comb}(t_j, S\sigma_{t_j})$$

where t_i and σ_{t_i} are the measured proper time and its error for event i. The proper-time probability distribution of the events in the peak consists of four components

$$\mathcal{P}_{peak} = f_{sig}\mathcal{P}_{sig} + f_{comb}\mathcal{P}_{comb} + f_{D_sD}\mathcal{P}_{D_sD} + f_{refl}\mathcal{P}_{refl}$$

Here:

- The probability density function $\mathcal{P}_{sig}$ of the B_s^0 signal is taken to be an exponential of lifetime τ_{B_s} convoluted with a Gaussian resolution function ($G(S\sigma_t)$) whose width is determined by the event-by-event error on the proper time σ_t scaled by the correction factor S discussed previously. The κ distribution is also numerically convoluted.
$$\mathcal{P}_{sig} = G(S\sigma_t) \otimes exp(t, \tau_{B_s}) \otimes \kappa.$$

- The probability density function $\mathcal{P}_{comb}$ of the combinatorial background is parametrized from the data by a fit to the side bands and is given by:
$$\mathcal{P}_{comb} = f_0 G(S\sigma_t) + f_1 G(S\sigma_t) \otimes exp(t, \tau_1) + (1 - f_0 - f_1) G(S\sigma_t) \otimes exp(t, \tau_2).$$
It consists of three components; a fraction f_0 of prompt (zero lifetime) background which is just the Gaussian resolution function and fractions f_1 and $1 - f_0 - f_1$ of two exponentials having lifetimes τ_1, τ_2 each convoluted with the same Gaussian resolution function.

- The probability density function $\mathcal{P}_{D_sD}$ of the D_sD background is taken to be an exponential of lifetime τ_{D_sD} convoluted with the Gaussian resolution function.
$$\mathcal{P}_{D_sD} = G(S\sigma_t) \otimes exp(t, \tau_{D_sD}).$$

As τ_{D_sD} cannot be measured in the data it is taken from a fit to the proper-time distribution observed in a Monte Carlo simulation of $B \to D_s DX$ events generated with the average b hadron lifetime (1.5 ps). After applying all the selection criteria this value is found to be $\tau_{D_sD} = 2.03^{+0.12}_{-0.11}$ ps. This effective lifetime is somewhat longer than the average b lifetime mainly because the boost is underestimated for these events. The error includes a variation range from 0.5 to 1.7 for the ratio of D^0 to D^+ yields in $B \to D_s DX$ decays, where the D is either a D^0 or a D^+ which decays semileptonically.

- The probability density function $\mathcal{P}_{refl}$ of the reflection background is taken to be an exponential of lifetime τ_{refl} convoluted with the Gaussian resolution function and the κ distribution.

$$\mathcal{P}_{refl} = G(S\sigma_t) \otimes exp(t, \tau_{refl}) \otimes \kappa.$$

The value of τ_{refl} is set to the average b hadron lifetime of 1.5 ps.

To improve the statistical error on the background parametrization coming from the side band events, the same-sign correlation events are also included in the "side band" sample. As the likelihoods for the peak and "side bands" are maximized simultaneously, the statistical error on the lifetimes of the combinatorial background is included in the statistical error of τ_{B_s}.

The relative fractions of the signal (f_{sig}) and the backgrounds (f_{comb}, f_{D_sD} and f_{refl}) are fixed in the fit and are taken from table 1. The free parameters in the fit are thus the B_s^0 lifetime (τ_{B_s}) and the shape of the combinatorial background as parametrized by f_0, f_1, τ_1 and τ_2.

6 Results of the Lifetime Fits

Figure 4a shows the proper time distribution of the events in the signal mass region of the opposite sign correlation events and the result of the lifetime fit. The fitted B_s^0 lifetime is

$$\tau_{B_s} = 1.92^{+0.45}_{-0.35} \text{ ps}$$

where the error is statistical only. Figure 4b shows the proper time distribution of the events in the "side band" mass regions and the result of the lifetime fit. The various contributions to the systematic errors for the B_s^0 lifetime are summarized in table 2.

Although the scaling factor S for the decay length error cannot be directly measured in real data for the exact decay topology used in this analysis, a check on the accuracy of the Monte Carlo to reproduce the data is possible using a "pseudo" resolution function constructed from the data by selecting events unlikely to have a secondary vertex in one hemisphere and then measuring the apparent decay length observed in the other hemisphere. To select these *uds* enriched events the hemisphere b tag described in reference [17] is used in veto mode and fake $D_s^- \ell^+$ combinations are formed in the opposite hemisphere using the same selection criteria as for the B_s^0 except that no lepton identification is required. The sigma of a Gaussian fit to the negative side of

Source of Systematic Error	Value (ps)
Uncertainty in tracking errors (S)	± 0.02
Combinatorial background	± 0.02
$D_s D$ background	± 0.02
$D_s X_s l\nu$ background	$^{+0.01}_{-0.00}$
Hadronic neutral energy	± 0.02
Higher mass $c\bar{s}$ states	± 0.01
Total in quadrature	± 0.04

Table 2: Summary of systematic errors for the B_s^0 lifetime.

the distribution of the measured decay length divided by its uncertainty is an estimate of S and yields a value of 1.20 ± 0.06. A similar procedure performed on Monte Carlo $q\bar{q}$ events yields a value 1.15 ± 0.04 indicating good agreement between the Monte Carlo and data for this quantity. For the possible systematic error coming from the uncertainty on the knowledge of S, it is varied $\pm 10\%$ about the value of 1.21 obtained in the Monte Carlo simulation of the signal events, leading to a change of ± 0.01 ps in the B_s^0 lifetime. To take into account the effect of possible tails in the resolution function this error is increased to ± 0.02 ps.

To estimate the systematic error from the parametrization of the proper-time distribution of the combinatorial background an alternative parametrization consisting of a single exponential was used. This yielded a lifetime change of -0.02 ps. Varying the estimate of the number of combinatorial background events within the statistical error coming from the mass fit changed the lifetime of the B_s^0 by ± 0.02 ps. This latter error is added in quadrature to the statistical error.

Varying the size of the $D_s D$ background and its effective lifetime within their uncertainties changed τ_{B_s} by ± 0.02 ps. Taking the maximum theoretical limit for the branching ratio $B \to D_s X_s l\nu$ and the efficiency measured in a Monte Carlo simulation of this decay, a maximum of 1.3 events (95% confidence limit) arising from this process may be present in the sample. Using an effective lifetime of 1.65 ± 0.24 ps obtained for these events in the simulation, the effect on the B_s^0 lifetime is ± 0.01 ps.

The neglect of the neutral hadronic energy in the estimate of the missing energy, as well as being partly responsible for the tail of the κ distribution (figure 3), introduces a systematic error in the neutrino energy measurement. To estimate this effect, the relative fraction of the tail was varied by $\pm 20\%$. This is a conservative upper limit on the uncertainty on the fraction of neutral hadronic energy in a hemisphere containing a high energy D_s^- and a lepton. It produces a variation of ± 0.02 ps in the B_s^0 lifetime.

The effect of B_s^0 decays to higher mass charm-strange states was investigated and estimated to contribute a systematic error of ± 0.01 ps. With the inclusion of the neutrino in the momentum estimate the sensitivity of the lifetimes to the assumed fragmentation and decay models is negligible. As the B_s^0 mass is well measured the systematic error from this source is also negligible.

To investigate the interpretation of the final error coming from the fit, 20,000

Monte Carlo experiments were produced with signal and background events generated according to the proper time distributions and number of events measured in this experiment. In these Monte Carlo experiments the total number of events in the signal peak was fixed to 47 and the number of background events allowed to vary within its statistical error according to a Poisson distribution. The bias on the lifetime arising from the use of the maximum likelihood method on a small statistical sample was found to be negligible and 69% of the experiments were found to be within one sigma of the error given by the fit. This study also shows that, if the true B_s^0 lifetime is 1.5 ps, the probability of measuring 1.92 ps or larger is 11%.

As a further consistency check, the lifetime of the D_s^- meson within the B_s^0 sample was also measured. The D_s^- decay length is calculated as the distance between the B_s^0 and D_s^- vertices. Using the same fitting method as described previously, except for the removal of the κ convolution, the maximum-likelihood fit to the data yields $\tau_{D_s} = 0.54^{+0.13}_{-0.10}$ ps in agreement with the world average value of $\tau_{D_s} = 0.45 \pm 0.03$ ps [1].

7 Conclusions

From a data sample of 889,000 hadronic Z events recorded with the ALEPH detector at LEP, 30.8 ± 6.9 events are attributed to the semileptonic decay of the B_s^0 to a D_s^- and an opposite-sign lepton. The proper times of these events are measured from their three-dimensional decay length and their relativistic boost estimated using a missing energy technique to account for the neutrino energy. A maximum-likelihood fit to the distribution of these proper times yields a B_s^0 lifetime of :

$$\tau_{B_s} = 1.92^{+0.45}_{-0.35} \pm 0.04 \text{ ps}.$$

This result is consistent with the B_s^0 lifetimes measured by the OPAL [18] and DELPHI collaborations [19] of $1.13^{+0.35}_{-0.26} \pm 0.09$ ps and 0.96 ± 0.37 ps respectively. It is also consistent with the average b lifetime of $\tau_b = 1.49 \pm 0.03 \pm 0.06$ ps measured by the ALEPH collaboration [20].

Acknowledgement

We wish to thank our colleagues in the CERN accelerator divisions for the successful operation of the LEP storage ring. We also thank the engineers and technicians in all our institutions for their support in constructing and operating ALEPH. Those of us from non-member states thank CERN for its hospitality.

References

[1] Particle Data Group, Phys. Rev. D 45 (1992).

[2] M. B. Voloshin and M. A. Shifman, Sov. Phys. JETP 64 (1986) 698.

[3] I.I.Bigi and N. Uraltsev, Phys. Lett. B 280 (1992) 271.

[4] DELPHI Collab., P. Abreu *et al.*, Phys. Lett. B 289 (1992) 199.

[5] ALEPH Collab., D. Buskulic *et al.*, Phys. Lett. B 294 (1992) 145.

[6] OPAL Collab., P.D. Acton *et al.*, Phys. Lett. B 295 (1992) 357.

[7] ALEPH Collab., D. Buskulic *et al.*, Phys. Lett. B 311 (1993) 425; erratum ibid. B 316 (1993) 631.

[8] CDF Collab., F. Abe *et al.*, Phys. Rev. Lett. 71 (1993) 1685.

[9] ALEPH Collab., D. Decamp *et al.*, Nucl. Instr. Meth. A294 (1990) 121.

[10] G. Batignani *et al.*, Conference Record of the 1991 IEEE Nuclear Science Symposium, Santa Fe, New Mexico, USA.

[11] ALEPH Collab., D. Decamp *et al.*, Phys. Lett. B 244 (1990) 551.
ALEPH Collab., D. Decamp *et al.*, Phys. Lett. B 263 (1991) 325.

[12] CLEO Collab., D. Bortoletto *et al.*, Phys. Rev. Lett. 64 (1990) 2117.

[13] ARGUS Collab., H. Albrecht *et al.*, Z. Phys. C 48 (1992) 1.

[14] ARGUS Collab., H. Albrecht *et al.*, Z. Phys. C 60 (1993) 11.

[15] E.Golowich *et al.*, Z. Phys. C 48 (1990) 89.

[16] ALEPH Collab., D. Buskulic *et al.*, Phys. Lett. B 307 (1993) 194.

[17] ALEPH Collab., D. Buskulic *et al.*, Phys. Lett. B 313 (1993) 535.

[18] OPAL Collab., P.D. Acton *et al.*, Phys. Lett. B 312 (1993) 501.

[19] DELPHI Collab., P. Abreu *et al.*, 'Production rate and Decay Lifetime Measurements of B_s^0 mesons at LEP using D_s and ϕ mesons', CERN-PPE/93-176.

[20] ALEPH Collab., D. Buskulic *et al.*, Phys. Lett. B 295 (1992) 174.

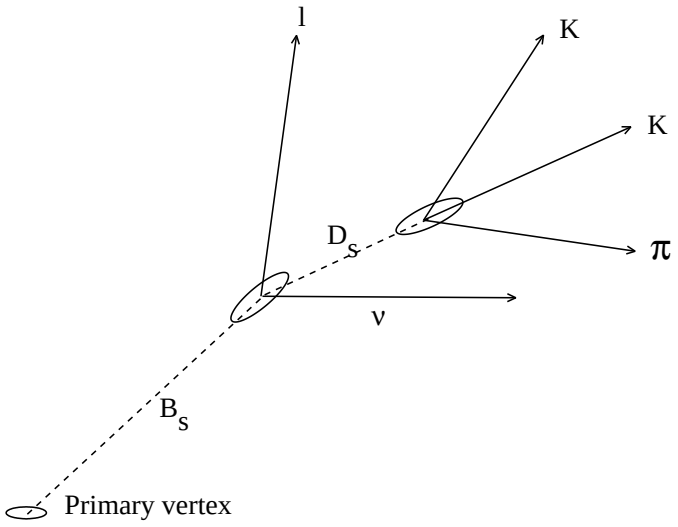

Figure 1: Typical decay topology of the events used for the B_s^0 lifetime measurement.

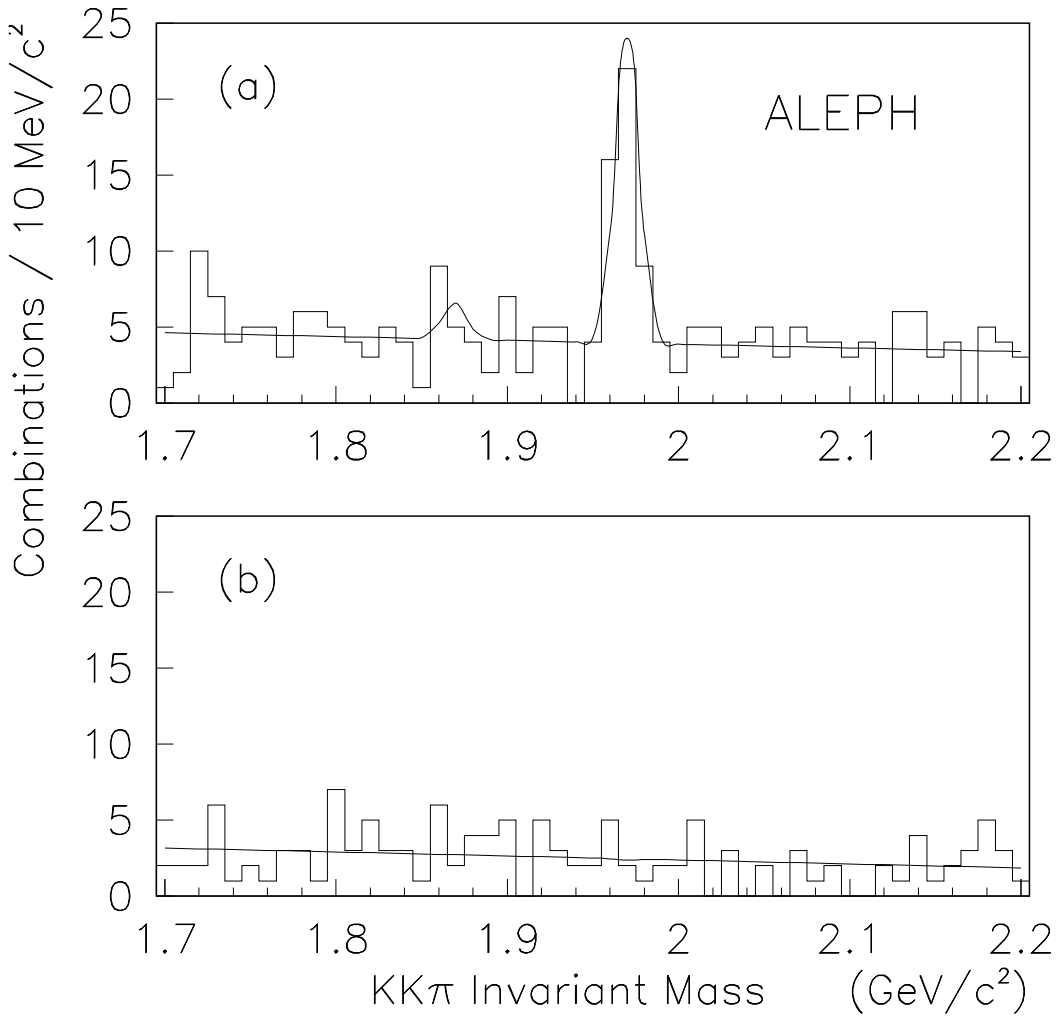

Figure 2: The $KK\pi$ effective mass for (a) opposite-sign and (b) same-sign D_s lepton correlation. The solid curve is a fit of the sum of a polynominal and two Gaussians at the D^- and D_s^- masses with the expected resolution.

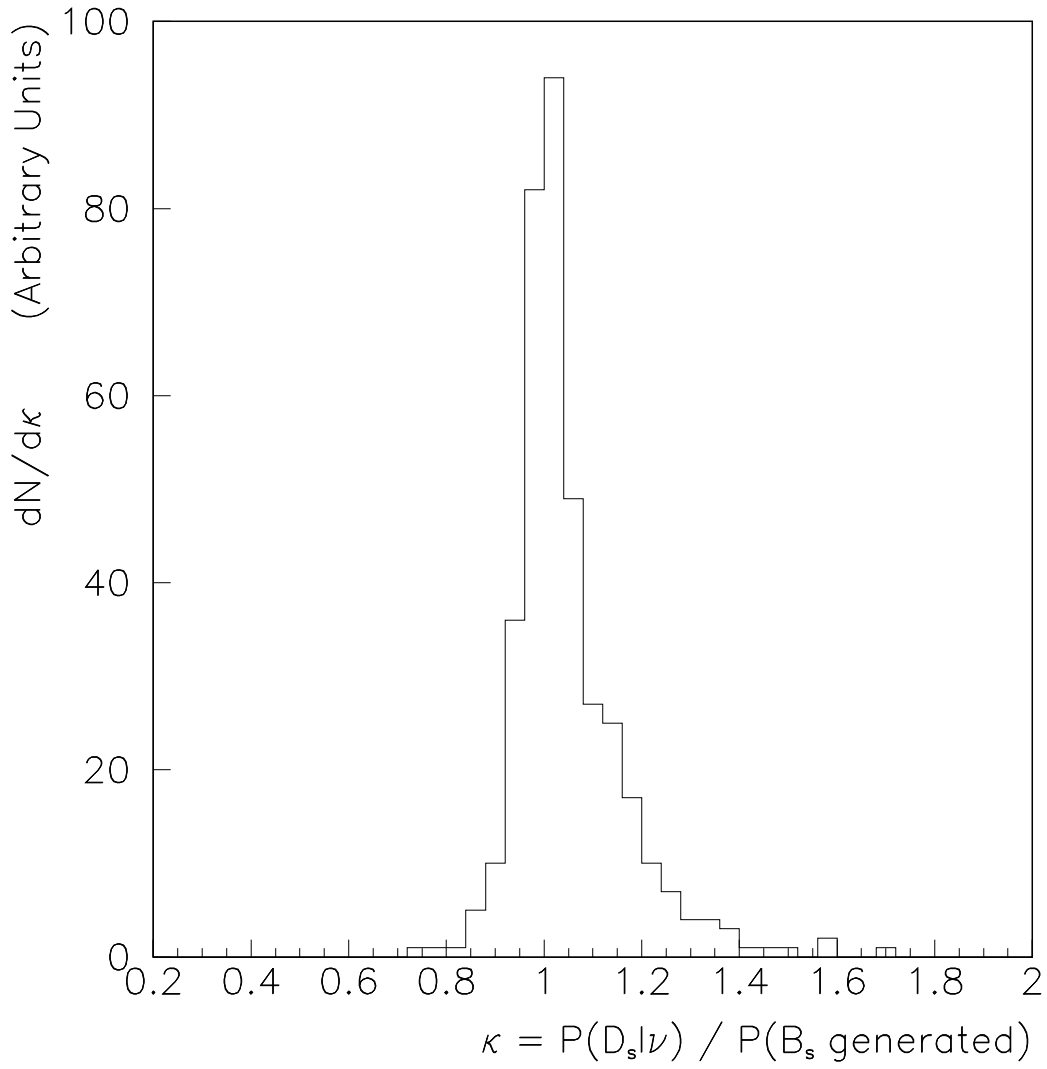

Figure 3: The distribution of the ratio of the reconstructed $D_s l\nu$ momentum to the true B_s momentum as obtained from Monte Carlo simulation.

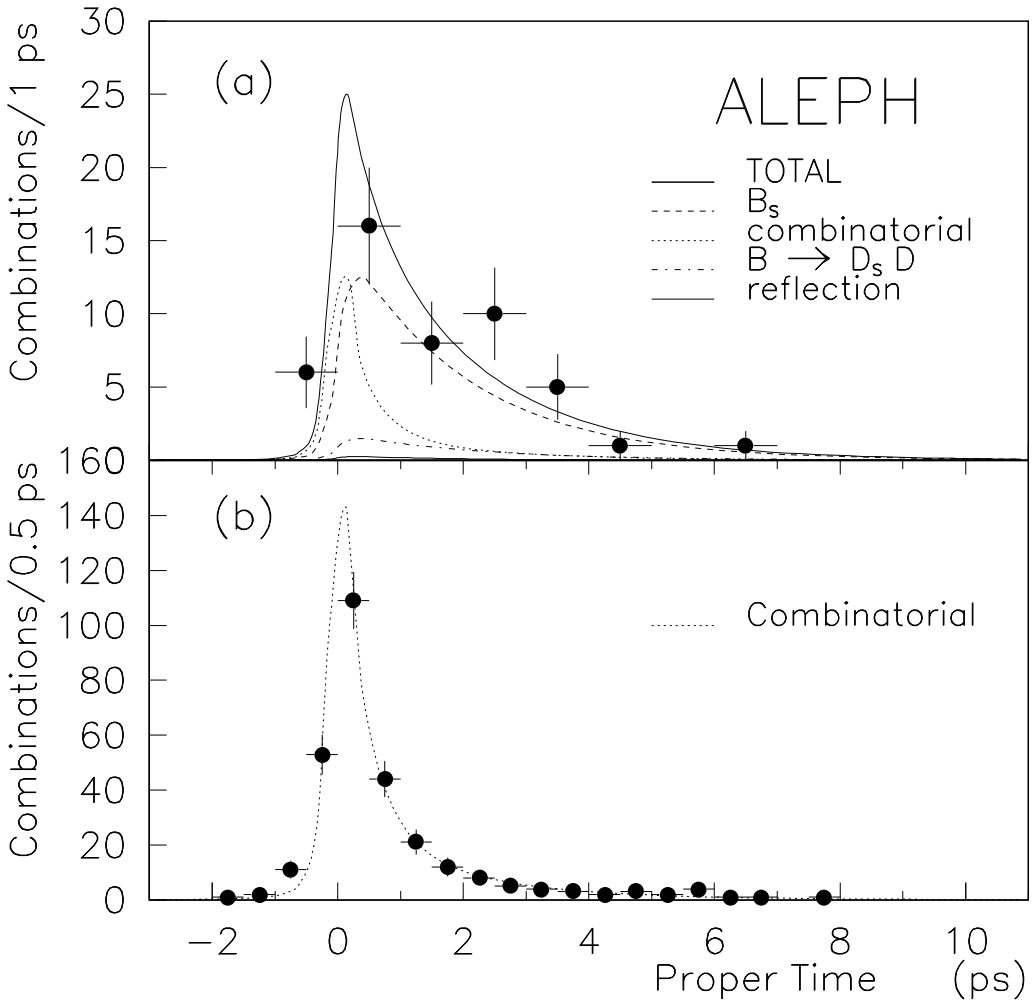

Figure 4: Result of the maximum likelihood fit to the proper-time distribution of (a) the D_s^- mass region of the opposite-sign $D_s^- l^+$ correlation events and (b) the side bands of the opposite-sign $D_s^- l^+$ and all of the same-sign $D_s^- l^-$ correlation events.